MITSUBISHI ELECTRIC RESEARCH LABORATORIES
https://www.merl.com

Joint Tire-Stiffness and Vehicle-Inertial Parameter Estimation for Improved Predictive Control

Berntorp, Karl; Quirynen, Rien; Vaskov, Sean

TR2021-060 June 04, 2021

Abstract

This paper presents a method for online estimation of linear friction (i.e., tire stiffness) and inertial parameters (i.e., mass and inertia) using sensors readily available from the CAN bus in production vehicles. We treat the tire stiffness as a timevarying Gaussian disturbance acting on the vehicle, and the inertial parameters are modeled as nearly constant parameters with large initial uncertainty. We leverage particle filtering and the marginalization concept to estimate in a computationally efficient way the tire-stiffness and inertial parameters, together with the vehicle state. We integrate the estimator with a nonlinear model-predictive controller (NMPC) and evaluate the efficacy of the estimator in closed-loop control.

American Control Conference

© 2021 MERL. This work may not be copied or reproduced in whole or in part for any commercial purpose. Permission to copy in whole or in part without payment of fee is granted for nonprofit educational and research purposes provided that all such whole or partial copies include the following: a notice that such copying is by permission of Mitsubishi Electric Research Laboratories, Inc.; an acknowledgment of the authors and individual contributions to the work; and all applicable portions of the copyright notice. Copying, reproduction, or republishing for any other purpose shall require a license with payment of fee to Mitsubishi Electric Research Laboratories, Inc. All rights reserved.

Mitsubishi Electric Research Laboratories, Inc.
201 Broadway, Cambridge, Massachusetts 02139

Joint Tire-Stiffness and Vehicle-Inertial Parameter Estimation for Improved Predictive Control

Karl Berntorp[1], Rien Quirynen[1], and Sean Vaskov[1]

Abstract— **This paper presents a method for online estimation of linear friction (i.e., tire stiffness) and inertial parameters (i.e., mass and inertia) using sensors readily available from the CAN bus in production vehicles. We treat the tire stiffness as a time-varying Gaussian disturbance acting on the vehicle, and the inertial parameters are modeled as nearly constant parameters with large initial uncertainty. We leverage particle filtering and the marginalization concept to estimate in a computationally efficient way the tire-stiffness and inertial parameters, together with the vehicle state. We integrate the estimator with a nonlinear model-predictive controller (NMPC) and evaluate the efficacy of the estimator in closed-loop control.**

I. Introduction

Inertial and road-surface properties are among the most important when assessing vehicle handling and performance characteristics. Automotive manufacturers can provide values for the inertial parameters. However, they are typically for some nominal (e.g., empty) loading conditions, whereas in reality the loading conditions will vary significantly between different drives. The interaction between road and vehicle is highly nonlinear and depends on several factors [1], and individual tires have different characteristics. To identify the nonlinear tire-force function, obtaining data is difficult as it requires to drive the vehicle to its performance limits.

The force-slip relation is approximately linear for small slip values. Hence, excluding at-the-limit maneuvers, it is reasonable to model the tire forces as proportional to the respective slip quantity. The proportionality constant is referred to as the tire stiffness. However, the tire stiffness and inertial parameters are tightly coupled, such that wrong estimates for, for example, the mass, will result in biased stiffness estimates [2]. This will affect the control performance, both in terms of constraint violations and vehicle stability, but also in terms of comfort and energy efficiency.

Model-predictive control (MPC) has become an established vehicle-control method [3]–[5]. As MPC exploits a vehicle model to perform predictions in its optimal control problem (OCP), the model should adequately represent the current vehicle behavior. A key issue in applying MPC to vehicle tracking control is in its combination with estimation algorithms to adjust the prediction model to the current environmental conditions. For instance, in challenging maneuvers it is imperative to have a well-informed guess about the surface on which the car is driving [4].

Previously, in [6], we developed a joint vehicle state and tire-stiffness estimator relying on inertial and wheel-speed sensing readily available from the CAN bus. In [5], we integrated the tire-stiffness estimator with a nonlinear MPC to provide friction adaptation within the MPC framework. However, a limitation with the tire-stiffness estimator in [6] is that it assumes fixed inertial parameters. If the inertial parameters used in the estimator are inaccurate, the estimates will be biased, which leads to degraded control performance.

This paper extends the particle-filter (PF) based tire-stiffness estimation method in [6] to include online adaptation to the mass and inertia of the vehicle. Both the mass and inertia enter the vehicle dynamics nonlinearly, which would motivate to treat the mass and inertia in the PF by augmenting the state. However, to enable a computationally efficient implementation, we leverage that for a standard passenger vehicle, the inertial parameters are large such that for small initial errors the nonlinear relation is approximately linear. Hence, we can solve for the mass and inertia by approximately marginalizing them out, which leads to an analytic solution that is locally accurate. We integrate the method into a nonlinaer MPC (NMPC) based on an efficient block-sparse quadratic program (QP) solver [7] for use within the real-time iteration (RTI) framework of nonlinear optimal control [8], and show that the inclusion of inertial parameter estimates in the NMPC formulation leads to significantly improved tracking performance compared to only adapting to the tire-stiffness estimates.

There is a large amount of prior work on estimation of inertial parameters and tire stiffness independently of each other, but the literature on joint estimation of tire stiffness and inertial parameters is limited. In [9], a recursive linear least-squares estimator with multiple forgetting factors for simultaneous estimation of the road grade and vehicle mass in real time was developed. The method in [2] is based on the multiple-model framework and considers tire stiffness, mass, and other parameters using a quite standard sensor setup. However, [2] does not consider that multiple-model estimation may be unsuitable for real-time control due to abrupt switching between models and the corresponding chattering behavior in the estimates. Our proposed method does not exhibit this behavior. For tire-stiffness estimation, many methods use sensors that are nonstandard in production vehicles or are not readily available from the CAN bus. A regression-based method is found in [10] and two methods for cornering stiffness estimation are described in [11], [12].

Notation: With $p(\boldsymbol{x}_{0:k}|\boldsymbol{y}_{0:k})$, we mean the posterior density function of the state trajectory $\boldsymbol{x}_{0:k}$ from time index 0 to time index k given the measurement sequence $\boldsymbol{y}_{0:k} := \{\boldsymbol{y}_0, \ldots, \boldsymbol{y}_k\}$. We write $\boldsymbol{f}_k$ for a function $\boldsymbol{f}(\boldsymbol{x}_k, \boldsymbol{u}_k)$,

[1]Mitsubishi Electric Research Laboratories (MERL), 02139 Cambridge, MA, USA. Email:karl.o.berntorp@ieee.org

where $\boldsymbol{u}$ is the input. For a vector $\boldsymbol{x}$, $\boldsymbol{x} \sim \mathcal{N}(\boldsymbol{\mu}, \boldsymbol{\Sigma})$ means that $\boldsymbol{x}$ is Gaussian distributed with mean $\boldsymbol{\mu}$ and covariance $\boldsymbol{\Sigma}$, and $|\boldsymbol{\Sigma}|$ is the determinant of $\boldsymbol{\Sigma}$. The notation $\mathcal{T}(\boldsymbol{\mu}, \boldsymbol{\Upsilon}, \nu)$ means the multivariate Student-t distribution with mean $\boldsymbol{\mu}$, scaling $\boldsymbol{\Upsilon}$, and ν degrees of freedom. Similarly, $\mathcal{NIW}(\gamma, \boldsymbol{\mu}, \boldsymbol{\Lambda}, \nu)$ reads the Normal-inverse-Wishart distribution with statistics (hyperparameters) summarized in $S := (\gamma, \boldsymbol{\mu}, \boldsymbol{\Lambda}, \nu)$. The notation $\hat{\boldsymbol{z}}_{k|m}$ denotes the estimate of $\boldsymbol{z}$ at time index k given measurements up to time index m.

II. Estimation Modeling

We summarize the estimation model and problem formulation. For details, see [6]. We model the vehicle by a single-track model [13], and assume that the left and right wheels on each axle have the same stiffness. Furthermore, we assume that the inertial parameters are slowly time varying and any large changes occur in discrete jumps. This is motivated by that substantial loading changes typically occur when the vehicle is at standstill and not during driving.

In the following, F^x, F^y are the longitudinal and lateral tire forces, respectively, α is the wheel-slip angle, ψ is the yaw, and subscripts f, r denote front and rear, respectively. With the state $\boldsymbol{x} = [v^X \; v^Y \; \dot{\psi}]^\top$, where v^X is the longitudinal vehicle velocity, v^Y is the lateral vehicle velocity, and $\dot{\psi}$ is the yaw rate, the equations of motion are

$$m(\dot{v}^X - v^Y\dot{\psi}) = F^X - F^y_f \sin(\delta), \tag{1a}$$

$$m(\dot{v}^Y + v^X\dot{\psi}) = F^y_f \cos(\delta) + F^y_r + F^x_f \sin(\delta), \tag{1b}$$

$$I\ddot{\psi} = l_f(F^y_f \cos(\delta) + F^x_f \sin(\delta)) - l_r F^y_r, \tag{1c}$$

where m is the unknown mass, I is the unknown inertia, and $F^X = F^x_f \cos(\delta) + F^x_r$. We assume that the tire force can be expressed as linear functions of the wheel slip λ and slip angle α, respectively,

$$F^x \approx C^x\lambda, \quad F^y \approx C^y\alpha, \tag{2}$$

where C^x and C^y are the longitudinal and lateral stiffness, respectively. We define λ_i and α_i as

$$\lambda_i = \frac{R_w\omega_i - v^x_i}{v^x_i}, \; \alpha_i = -\arctan\left(\frac{v^y_i}{v^x_i}\right), \tag{3}$$

where $i \in \{f, r\}$, ω_i is the wheel rotation rate, v^x_i and v^y_i are the longitudinal and lateral wheel velocities for wheel i with respect to an inertial system, in the coordinate system of the respective wheel, and R_w is the effective wheel radius.

The complete vehicle model (1)–(3) is nonlinear in v^X and v^Y and the inertial parameters $\bar{\boldsymbol{m}} = [m \; I]^\top$. There are also bilinearities between both states, and states and parameters. Considering both longitudinal and lateral dynamics allows to account for the coupling in (1), but increases computational burden. The wheel rotation rates ω_f, ω_r and the steer angle δ form the input vector $\boldsymbol{u}$, which is assumed known.

Remark 1. *In the remainder of this paper we focus on determining the lateral (i.e., cornering) stiffnesses jointly with the inertial parameters, since the cornering stiffness is more important than the longitudinal stiffness for vehicle-stability control. However, the longitudinal case can be treated using the same framework, see [6].*

A. Estimation Model

To establish the estimation model, focusing on the lateral dynamics, we decompose the stiffness parameters into one known nominal part and one unknown part,

$$C^y = C^y_n + \Delta C^y, \tag{4}$$

where C_n is the nominal value of the stiffness, for example, a priori determined on a nominal surface, and ΔC is a time-varying, unknown part. We define $\boldsymbol{w}_k := \begin{bmatrix}\Delta C^y_f & \Delta C^y_r\end{bmatrix}^\top$ as random process noise acting on the otherwise deterministic system. We model the noise term $\boldsymbol{w}_k$ as Gaussian distributed according to $\boldsymbol{w}_k \sim \mathcal{N}(\boldsymbol{\mu}_k, \boldsymbol{\Sigma}_k)$, where $\boldsymbol{\mu}_k$ and $\boldsymbol{\Sigma}_k$ are the unknown, usually time varying, mean and covariance. With the decomposition (4) and after discretization of the continuous-time vehicle model (1)–(3),

$$\boldsymbol{x}_{k+1} = \boldsymbol{f}(\boldsymbol{x}_k, \bar{\boldsymbol{m}}_k, \boldsymbol{u}_k) + \boldsymbol{g}(\boldsymbol{x}_k, \bar{\boldsymbol{m}}_k, \boldsymbol{u}_k)\boldsymbol{w}_k. \tag{5}$$

Hence, the vehicle dynamics naturally leads to an interpretation of the unknown part of the tire stiffness as a process disturbance with unknown mean and covariance, which motivates a noise-adaptive approach.

We estimate both the state $\boldsymbol{x}_k$, the parameters $\boldsymbol{\mu}_k, \boldsymbol{\Sigma}_k$ (i.e., the mean and variance of the process noise $\boldsymbol{w}_k$), and the inertial parameters $\bar{\boldsymbol{m}}$. The loading conditions for a vehicle can have large variations between drives, but fuel consumption is the main cause for loading variations while driving. Hence, it is appropriate to model the inertial parameters as random walks with large initial uncertainty and Gaussian process noise. The measurements $\boldsymbol{y}$ are the longitudinal and lateral acceleration, a^X, a^Y, and yaw rate $\dot{\psi}$.

Automotive-grade inertial sensors have errors $\boldsymbol{b}$, which can be significant over long time periods. The error terms are both additive (bias) and multiplicative (scaling offsets). We assume that these bias terms are cancelled out a priori (see, e.g., [14]). The measurement model can be written as

$$\boldsymbol{y}_k = \boldsymbol{h}(\boldsymbol{x}_k, \bar{\boldsymbol{m}}_k, \boldsymbol{u}_k) + \boldsymbol{d}(\boldsymbol{x}_k, \bar{\boldsymbol{m}}_k, \boldsymbol{u}_k)\boldsymbol{w}_k + \boldsymbol{e}_k, \tag{6}$$

where $\boldsymbol{e}_k \in \mathbb{R}^{n_e}$, is the Gaussian zero-mean noise from the inertial sensors, $\boldsymbol{e}_k \sim \mathcal{N}(\boldsymbol{0}, \boldsymbol{R})$, where $\boldsymbol{R}$ is determined a priori. The joint Gaussian distribution of the tire-stiffness parameters $\boldsymbol{w}_k$ and measurement noise $\bar{\boldsymbol{e}}_k$ can be written as

$$\bar{\boldsymbol{w}}_k = \begin{bmatrix}\boldsymbol{w}_k^\top & \bar{\boldsymbol{e}}_k^\top\end{bmatrix}^\top \sim \mathcal{N}\left(\bar{\boldsymbol{\mu}}_k, \bar{\boldsymbol{\Sigma}}_k\right),$$

where we have introduced the short-hand notation $\bar{\boldsymbol{e}}_k = \boldsymbol{d}(\boldsymbol{x}_k, \bar{\boldsymbol{m}}_k, \boldsymbol{u}_k)\boldsymbol{w}_k + \boldsymbol{e}_k$, and where

$$\bar{\boldsymbol{\mu}}_k = \begin{bmatrix}\boldsymbol{\mu}_k \\ \boldsymbol{d}_k\boldsymbol{\mu}_k\end{bmatrix}, \tag{7a}$$

$$\bar{\boldsymbol{\Sigma}}_k = \begin{bmatrix}\boldsymbol{\Sigma}_k & \boldsymbol{\Sigma}_k\boldsymbol{d}_k^\top \\ \boldsymbol{d}_k\boldsymbol{\Sigma} & \boldsymbol{d}_k\boldsymbol{\Sigma}_k\boldsymbol{d}_k^\top + \boldsymbol{R}\end{bmatrix}, \tag{7b}$$

and $\boldsymbol{d}_k := \boldsymbol{d}_k(\boldsymbol{x}_k, \bar{\boldsymbol{m}}_k, \boldsymbol{u}_k)$. Thus, due to the use of inertial sensing, the noise sources with the structure given by (7b) are dependent. In this work, we estimate the process-noise statistics $\boldsymbol{\mu}_k$ and $\boldsymbol{\Sigma}_k$, which are embedded in (7), together with the inertial parameters $\bar{\boldsymbol{m}}$, and the state trajectory.

Remark 2. *If there is additional sensing, for example, from the suspension system effectively measuring the normal force, the estimation problem is significantly simplified since we then have measurements of the mass that are independent of the stiffness, whereas currently due to the inertial sensing, the mass and stiffness are coupled through the acceleration.*

Remark 3. *In this paper we only estimate the lateral tire stiffness and assume the longitudinal stiffness to be determined completely by the lateral stiffness as $C_i^x \approx 2C_i^y$. This approximation provides a coarse update of the longitudinal stiffness without introducing additional parameters into the tire-stiffness estimator. The linear relationship is based on the models used in simulation and could alternatively be fit with experimental data. Since the maneuvers in this work do not require large longitudinal accelerations, accurately modeling the longitudinal stiffness is not critical for performance.*

B. Observability

There are several ways to investigate observability for the present estimation model. A straightforward approach is to investigate nonsingularity of the observability Gramian. This can be done locally by defining the state vector

$$\bar{\boldsymbol{x}} = \begin{bmatrix} \boldsymbol{x}^\top & \boldsymbol{\mu}^\top & \bar{\boldsymbol{m}}^\top \end{bmatrix}^\top, \tag{8}$$

linearizing the system for different pairs of inputs and states, and checking the rank conditions. For nonzero inputs and velocities, by using exponential forgetting in the stiffness parameter estimation (see Sec. III), the observability Gramian is nonsingular and hence the system is weakly observable.

III. Marginalized Noise-Adaptive Particle Filtering for Inertial Estimation

In this section, we present our method for determining jointly the vehicle state $\boldsymbol{x}$, tire-stiffness parameters $\boldsymbol{\theta} := \{\boldsymbol{\mu}, \boldsymbol{\Sigma}\}$, and inertial parameters $\bar{\boldsymbol{m}}$. For space limitations, the parts on determining the vehicle state and tire stiffness are briefly summarized, and the details are in [6]. We approach our estimation problem by estimating the density $p(\bar{\boldsymbol{m}}_k, \boldsymbol{\theta}_k, \boldsymbol{x}_{0:k}|\boldsymbol{y}_{0:k})$, that is, the joint posterior conditioned on all measurements from time step 0 to k. We decompose

$$\begin{aligned} p(\bar{\boldsymbol{m}}_k, \boldsymbol{\theta}_k, \boldsymbol{x}_{0:k}|\boldsymbol{y}_{0:k}) &= p(\bar{\boldsymbol{m}}_k|\boldsymbol{\theta}_k, \boldsymbol{x}_{0:k}, \boldsymbol{y}_{0:k}) \\ &\quad \cdot p(\boldsymbol{\theta}_k|\boldsymbol{x}_{0:k}, \boldsymbol{y}_{0:k}) p(\boldsymbol{x}_{0:k}|\boldsymbol{y}_{0:k}). \end{aligned} \tag{9}$$

The three densities on the right-hand side of (9) are estimated recursively. The third term on the right-hand side is given by the particle filter. The key idea is that given the state trajectory, we can update the distribution of the noise parameters, that is, the second distribution on the right-hand side of (9). Given the tire stiffness and the state trajectory, we can approximately solve for the inertial parameters.

We approximate the state posterior using a PF as [15]

$$p(\boldsymbol{x}_{0:k}|\boldsymbol{y}_{0:k}) \approx \sum_{i=1}^{N} q_k^i \delta(\boldsymbol{x}_{0:k} - \boldsymbol{x}_{0:k}^i), \tag{10}$$

where $\delta(\cdot)$ is the Dirac delta mass, N is the number of particles, and q_k^i is the importance weight for the ith state trajectory $\boldsymbol{x}_{0:k}^i$. The particles are sampled from a proposal distribution $\pi(\boldsymbol{x}_{k+1}|\boldsymbol{x}_{0:k}^i, \boldsymbol{y}_{0:k+1})$. In this paper, we choose the proposal according to the motion model $p(\boldsymbol{x}_k^i|\boldsymbol{x}_{0:k-1}^i, \boldsymbol{y}_{0:k-1})$, which implies the weight update

$$q_k^i \propto q_{k-1}^i p(\boldsymbol{y}_k|\boldsymbol{x}_{0:k}^i, \boldsymbol{y}_{0:k-1}). \tag{11}$$

In our setting, since the unknown process-noise parameters affect both the measurement and prediction step, the prediction density and likelihood have to be adjusted accordingly. To estimate the tire stiffness (i.e., the process noise statistics) efficiently, we rely on conjugate priors [16], [17]. Given a likelihood, the conjugate prior is the prior distribution such that the prior and posterior are in the same family of distributions. Thus, for a conjugate prior, the prior and posteriors are of the same type, and the estimation problem simplifies to updating the hyperparameters. Given the state, the measurement likelihood is a multivariate Gaussian distribution, and for multivariate Normal data $\bar{\boldsymbol{w}} \in \mathbb{R}^d$ with unknown mean $\boldsymbol{\mu}$ and covariance $\boldsymbol{\Sigma}$, a Normal-inverse-Wishart distribution defines the conjugate prior $p(\boldsymbol{\mu}_k, \boldsymbol{\Sigma}_k) := \mathcal{NIW}(\gamma_{k|k}, \hat{\boldsymbol{\mu}}_{k|k}, \boldsymbol{\Lambda}_{k|k}, \nu_{k|k})$ by

$$\begin{aligned} \boldsymbol{\mu}_k|\boldsymbol{\Sigma}_k &\sim \mathcal{N}(\hat{\boldsymbol{\mu}}_{k|k}, \gamma_{k|k}\boldsymbol{\Sigma}_k), \\ \boldsymbol{\Sigma}_k &\sim \mathcal{IW}(\nu_{k|k}, \boldsymbol{\Lambda}_{k|k}) \\ &\quad \propto |\boldsymbol{\Sigma}_k|^{-\frac{1}{2}(\nu_{k|k}+d+1)} e^{\left(-\frac{1}{2}\mathrm{tr}(\boldsymbol{\Lambda}_{k|k}\boldsymbol{\Sigma}_k^{-1})\right)} \end{aligned}$$

where $\mathrm{tr}(\cdot)$ is the trace operator. The statistics $S_{k|k} := (\gamma_{k|k}, \hat{\boldsymbol{\mu}}_{k|k}, \boldsymbol{\Lambda}_{k|k}, \nu_{k|k})$ can be updated recursively [6], and a forgetting factor $\lambda \in [0, 1]$ is introduced that allows the estimator to discard older data. Further, for a Normal-inverse-Wishart prior, the predictive distribution of the data $\bar{\boldsymbol{w}}$ is a Student-t,

$$\mathrm{St}(\hat{\boldsymbol{\mu}}_{k|k-1}, \tilde{\boldsymbol{\Lambda}}_{k|k-1}, \nu_{k|k-1} - d + 1), \tag{12}$$

with

$$\tilde{\boldsymbol{\Lambda}}_{k|k-1} = \frac{1 + \gamma_{k|k-1}}{\nu_{k|k-1} - d + 1} \boldsymbol{\Lambda}_{k|k-1}.$$

This is utilized when sampling the process noise and evaluating the particles according to the measurement likelihood [6].

A. Mass and Inertia Estimation

The mass and inertia estimation update relies on having computed both the posterior for the state trajectory and the noise parameters. Thus, the estimation is concerned with computing the posterior $p(\bar{\boldsymbol{m}}_k|\boldsymbol{\theta}_k, \boldsymbol{x}_{0:k}, \boldsymbol{y}_{0:k})$, based on the following observations. First, the prediction model of the inertial parameters is a random walk, which is linear and Gaussian. Second, the dynamics of the mass and inertia are nonlinearly dependent on both the unknown process noise and the vehicle states. Third, the inertia does not enter the measurement equations. This has a few implications. First, we cannot exactly marginalize out the inertial parameters from the vehicle model. However, locally the nonlinearity is well represented by its first-order linearization. Hence, what we effectively are implementing is a Rao-Blackwellized PF (RBPF) by local approximations of the inertial parameters, with extended Kalman filters (EKFs) for each particle. Second, because we only have measurements of the yaw rate and lateral acceleration in our setup, the inertia is not part of the measurement model. Hence, the only information about the inertia comes from (1c), which acts as an extra measurement to the EKF. This extra step in the RBPF is crucial for the method to work. For the prediction step, since the prediction model is linear (random walk) with Gaussian process noise with covariance $\boldsymbol{Q}$, for each particle i,

$$\begin{aligned}
\hat{\bar{\boldsymbol{m}}}^i_{k+1|k} &= \boldsymbol{A}\hat{\bar{\boldsymbol{m}}}^i_{k|k} + \boldsymbol{L}^i_k(\boldsymbol{z}^i_k - (A^n)^i \hat{\bar{\boldsymbol{m}}}^i_{k|k}), \\
\boldsymbol{P}^i_{k+1} &= \boldsymbol{A}\boldsymbol{P}^i_k \boldsymbol{A}^\top + \boldsymbol{Q} - \boldsymbol{L}^i_k \boldsymbol{N}^i_k \boldsymbol{L}^{i,\top}_k, \\
\boldsymbol{N}^i_k &= (\boldsymbol{A}^n)^i \boldsymbol{P}^i_{k|k} (\boldsymbol{A}^n)^{i,\top} + \boldsymbol{d}^i_k \hat{\boldsymbol{\Sigma}}^i_{k|k} \boldsymbol{d}^{i,\top}_k, \\
\boldsymbol{L}^i_k &= \boldsymbol{A}\boldsymbol{P}^i_{k|k} (\boldsymbol{A}^n)^{i,\top} (\boldsymbol{N}^i)^{-1}_k, \\
\boldsymbol{z}^i_k &= \boldsymbol{x}^i_{k+1} - \boldsymbol{f}^i_k - \boldsymbol{g}^i_k \boldsymbol{\mu}^i_k, \\
(\boldsymbol{A}^n)^i &= \left.\frac{\partial \boldsymbol{f}^i}{\partial \boldsymbol{m}}\right|_{\boldsymbol{m} = \hat{\bar{\boldsymbol{m}}}^i_{k|k}},
\end{aligned} \tag{13}$$

where $\hat{\boldsymbol{\Sigma}}_{k|k} = \boldsymbol{\Lambda}^i_{k|k}/(\nu_{k|k} - 4)$. Since we know that the mass and inertia are tightly connected, we set the cross term to $Q_{12} = Q_{21} = \kappa\sqrt{(Q_{11}Q_{22})}$ for some $0 \ll \kappa < 1$. This enforces the estimator to correlate an increased mass with an increased inertia, and vice versa. For the measurement update, we have the regular EKF update, per particle, as

$$\begin{aligned}
\hat{\bar{\boldsymbol{m}}}^i_{k|k} &= \hat{\bar{\boldsymbol{m}}}^i_{k|k-1} + \boldsymbol{K}_k(\boldsymbol{y}_k - \boldsymbol{h}^i_k - \boldsymbol{d}^i_k \hat{\boldsymbol{\mu}}^i_{k|k} - \hat{\bar{\boldsymbol{m}}}^i_{k|k-1}), \\
\boldsymbol{K}^i_k &= \boldsymbol{P}^i_{k|k-1}(\boldsymbol{C}^i)^\top (\boldsymbol{S}^i_k)^{-1}, \\
\boldsymbol{P}^i_{k|k} &= (\boldsymbol{I} - \boldsymbol{K}^i_k \boldsymbol{C}^i)\boldsymbol{P}^i_{k|k-1}, \\
\boldsymbol{S}^i_k &= \boldsymbol{C}^i \boldsymbol{P}^i_{k|k-1}(\boldsymbol{C}^i)^\top + \boldsymbol{R} + \boldsymbol{d}^i_k \hat{\boldsymbol{\Sigma}}^i_{k|k}(\boldsymbol{d}^i_k)^\top, \\
\boldsymbol{C}^i &= \left.\frac{\partial \boldsymbol{h}}{\partial \bar{\boldsymbol{m}}}\right|_{\bar{\boldsymbol{m}} = \hat{\bar{\boldsymbol{m}}}^i_{k|k-1}}.
\end{aligned} \tag{14}$$

Algorithm 1 summarizes the method.

Remark 4. *We utilize the connection between mass and inertia by cross-correlated process noise and initial covariance. However, since the process noise is small in practice, the major effect comes from the initial covariance. To improve performance further, the relation* $I = \int \rho \|\boldsymbol{r}\|^2 \mathrm{d}V$ *can be used to derive an explicit connection between mass and inertia, either analytically for a simplified shape or numerically by look-up tables.*

Algorithm 1 Pseudo-code of the estimation algorithm

Initialize: Set $\{\boldsymbol{x}^i_0\}^N_{i=1} \sim p_0(\boldsymbol{x}_0)$, $\{q^i_0\}^N_{i=1} = 1/N$, $\{S^i_0\}^N_{i=1} = \{\gamma^i_0, \boldsymbol{\mu}^i_0, \boldsymbol{\Lambda}^i_0, \nu^i_0\}$, $\{\bar{\boldsymbol{m}}^i_0\}^N_{i=1} \sim p_0(\bar{\boldsymbol{m}}_0)$

for $k \leftarrow 0$ to T **do**
- **for each particle** $i \in \{1, \dots, N\}$ **do**
  - Update weight using (11).
  - Update noise statistics $S^i_{k|k}$ according to [6].
- **end for**
- Normalize weights as $q^i_k = \bar{q}^i_k / (\sum^N_{i=1} \bar{q}^i_k)$.
- Compute $N_{\text{eff}} = 1/(\sum^N_{i=1} (q^i_k)^2)$
- **if** $N_{\text{eff}} \leq N_{\text{thr}}$ **then**
  - Resample particles and copy the corresponding statistics. Set $\{q^i_k\}^N_{i=1} = 1/N$.
- **end if**
- Compute estimates of noise parameters.
- **for each particle** $i \in \{1, \dots, N\}$ **do**
  - Update mass and inertia using (14).
  - Predict noise statistics $S^i_{k+1|k}$ according to [6].
  - Sample $\boldsymbol{w}^i_k$ from (12).
  - Predict state $\boldsymbol{x}^i_{k+1}$ using (5).
  - Predict mass and inertia using (13).
- **end for**

end for

IV. NONLINEAR MPC FOR REAL-TIME VEHICLE CONTROL

The control inputs are the front road wheel steering angle rate of change command $\dot{\delta}$ and the front and rear wheel speeds ω_f and ω_r, respectively. We design a control strategy that makes the vehicle motion follow a time-dependent reference trajectory $\boldsymbol{y}_{\text{ref}} = (p^{\mathbf{X}}_{\text{ref}}, p^{\mathbf{Y}}_{\text{ref}}, \psi_{\text{ref}}, v^X_{\text{ref}})$, possibly generated in real time with an adequate preview, while operating over different surfaces and environmental conditions. The system dynamics are those given in Sec. II, appended with differential equations for the position, heading, and steering-wheel angle. We introduce the following tracking-type optimal control problem formulation in continuous time,

$$\min_{\boldsymbol{x}(\cdot),\, \boldsymbol{u}(\cdot)} \int_0^T \|\boldsymbol{F}(\boldsymbol{x}(t), \boldsymbol{u}(t)) - \boldsymbol{y}_{\text{ref}}(t)\|^2_{\boldsymbol{W}} \,\mathrm{d}t \tag{15a}$$

$$\text{s.t.} \quad 0 = \boldsymbol{x}(0) - \hat{\boldsymbol{x}}_0, \tag{15b}$$

$$\dot{\boldsymbol{x}}(t) = \boldsymbol{f}_{\boldsymbol{\theta}^*}(\boldsymbol{x}(t), \boldsymbol{u}(t)), \quad \forall t \in [0, T], \tag{15c}$$

$$0 \geq \boldsymbol{h}(\boldsymbol{x}(t), \boldsymbol{u}(t)), \quad \forall t \in [0, T], \tag{15d}$$

$$0 \geq r(\boldsymbol{x}(T)), \tag{15e}$$

where $\boldsymbol{x}(t) \in \mathbb{R}^{n_x}$ denotes the differential states and $\boldsymbol{u}(t) \in \mathbb{R}^{n_u}$ are the control inputs for $t \in [0, T]$, and where $\boldsymbol{\theta}^*$ are the set of tire stiffness and inertial parameters. For our particular setup $n_x = 7$ and $n_u = 3$, and we include an auxiliary slack variable to treat state-dependent inequality constraints as discussed in [5]. The objective in (15a) consists of a nonlinear least-squares type Lagrange term and an L1 penalty on the slack variable. For simplicity, T denotes both the control and prediction horizon length and we do not consider a terminal cost term. Note that the NMPC problem depends on the current state estimate $\hat{\boldsymbol{x}}_0$ through Eq. (15b).

The path constraints (15d) in the NMPC problem formulation consist of geometric and physical limitations of the system, such as constraints on the vehicle position. In practice, it is important to reformulate these requirements as soft constraints since otherwise the problem may become infeasible, for instance due to unknown disturbances and modeling errors. In this paper, we define an exact L1 penalty on the slack variable to ensure feasibility, similar to [3]. For the specific constraints, see [18].

A. Implementation Aspects

The nonlinear, nonconvex problem (15) renders analytical solutions intractable. Instead, we transform the infinite dimensional OCP (15) into a nonlinear program (NLP) by a control and state parameterization. To this end, we formulate an equidistant grid over the control horizon consisting of the collection of time points t_i, where $t_{i+1} - t_i = \frac{T}{N} =: T_s$ for $i = 0, \ldots, N-1$. Additionally, we consider a piecewise constant control parametrization $u(\tau) = \boldsymbol{u}_i$ for $\tau \in [t_i, t_{i+1})$. The time discretization for the state variables can then be obtained by simulating the system dynamics using a numerical integration scheme. This corresponds to solving the following initial value problem

$$\dot{\boldsymbol{x}}(\tau) = \boldsymbol{f}_{\boldsymbol{\theta}^*}(\boldsymbol{x}(\tau), \boldsymbol{u}_i), \quad \tau \in [t_i, t_{i+1}], \quad \boldsymbol{x}(t_i) = \boldsymbol{x}_i. \quad (16)$$

We employ a tailored implementation using the open-source ACADO Toolkit [8]. The nonlinear optimal control solver in this toolkit uses an online variant of SQP, known as the RTI scheme [19]. Under some reasonable assumptions, the stability of the closed-loop system based on the RTI scheme can be guaranteed also in presence of inaccuracies and external disturbances [19]. ACADO Toolkit exports efficient, standalone C-code implementing the RTI scheme for fast optimal control. Specifically, we use the recently proposed PRESAS QP solver [4], [7], which applies block-structured factorization techniques with low-rank updates to preconditioning of an iterative solver within a primal active-set algorithm. This results in an efficient QP solver suitable for embedded automotive applications. A primal active-set approach has the advantage of providing a feasible, even though suboptimal, solution when being terminated early.

V. Simulation Results

First, we simulate a sinusoidal steering maneuver to see the estimation performance under sufficient persistence of excitation. In the second simulation, we close the loop with the NMPC, where we want to perform a double lane-change maneuver when there is an abrupt change in road surface.

The vehicle parameters are from a mid-size SUV, and the tire parameters for the different surfaces are the same as in [18]. The tire-stiffness estimator uses $N = 500$ particles and the inertial sensor measurement noise values are taken from those of a low-cost inertial measurement unit common in automotive applications. The initial estimates and the different tuning parameters for the tire-stiffness part are generic and the same as in [6].

A. Estimation Performance Evaluation

For the first results, we have simulated a sinusoidal steering maneuver for 50 seconds with constant velocity data (40 km/h). Fig. 1 shows the inertial estimates averaged over 50 Monte-Carlo runs when driving on asphalt with a sudden change to snow. The gray filled area is the 2σ spread of the estimates over the executions. We set the mean of the initial guess of the stiffness estimates to be in between the true values for snow and asphalt, and the mass and inertia have an initial covariance matrix $\boldsymbol{P}_0 = [200, 100; 100, 400]$. Note that for the case of having correct inertial parameters, we have previously shown that the estimator is unbiased, even for experimental data [6]. The mass estimates converge accurately, but there is a bias in the inertia. This is unsurprising, since the only information we get about the inertia is from the states, not from the actual measurements, and the filter executes with 500 particles.

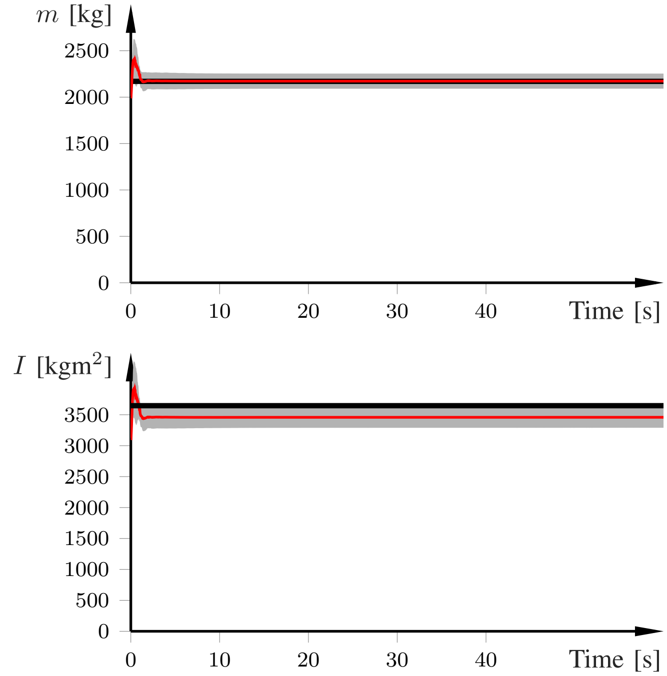

Fig. 1. Mass and inertia results for 50 Monte-Carlo executions on surface change from asphalt to snow at $t = 30$s for sinusoidal steering maneuvers.

B. Closed-Loop Control Performance

Here, the vehicle tracks nine double lane-change and return maneuvers, with the middle three on snow and the rest on dry asphalt. The maneuver is reminiscent of the standardized IS0 3888-2 maneuver. The tire-stiffness and inertial parameter estimates are fed into the NMPC. On the other hand, the simulation model uses a nonlinear Pacejka tire model and the friction ellipse to model combined slip [1], [20]. The reference velocity is fixed to 19 m/s. The reference is generated with Bezier polynomials and the position, heading, longitudinal velocity, and yaw rate are given to the controllers to track. The lateral constraints we enforce are that the vehicle is not allowed to leave the road boundaries. We compare the following controllers: STIFFNESS, an NMPC with the tire-stiffness estimator in [6]; PROPOSED, the proposed method with both tire-stiffness and inertial parameter estimation; ORACLE, which uses an NMPC with the true nonlinear tire-force model and correct inertial parameters (this controller acts as ground truth and cannot be implemented in practice); SNOW, an NMPC that uses the correct inertial parameters but snow stiffness values; ASPHALT, an NMPC that uses the correct inertial parameters but asphalt stiffness values. All controllers perform 1 SQP iteration per planning step. The estimator is executed at 100Hz and the MPC at 20Hz. The metrics to evaluate

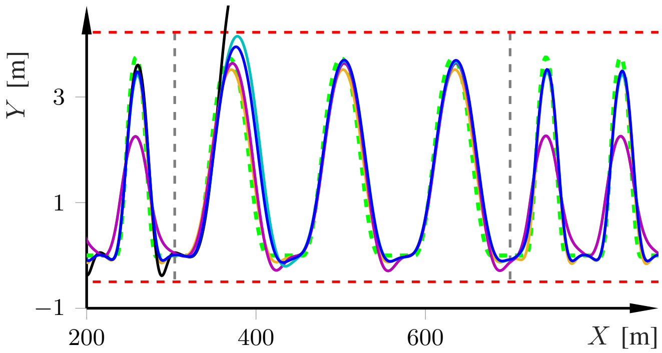

Fig. 2. Resulting path for the various approaches during the lane-change maneuvers. Red and green dashed lines are the constraints and reference, respectively. The gray vertical dashed line indicates the surface change from asphalt to snow. The blue, cyan, magenta, black, and gold lines indicate the trajectories for PROPOSED, STIFFNESS, SNOW, ASPHALT, and ORACLE.

TABLE I

RESULTS FOR 100 MONTE-CARLO RUNS FOR THE MANEUVER IN FIG. 2.

Method	Mean Cost	Max Cost	Mean Score	Max Score
STIFFNESS	3.144	6.879	0.051	0.077
PROPOSED	2.091	6.546	0.010	0.035
ORACLE	0.699	0.700	0	0
SNOW	3.344	3.361	0	0
ASPHALT	203.399	256.583	6.107	6.473

the controllers are cost, Cost $= \sum_k l(\boldsymbol{x}_k, \boldsymbol{u}_k)$, and score, Score $= \sum_k ((y_k - y_{\max})_+ + (y_{\min} - y_k)_+)\, t_s$, summed over the simulation time, where $(\cdot)_+ = \max(\cdot, 0)$ and $l(\cdot)$ is defined by the MPC objective function.

Fig. 2 shows the lateral tracking performance for one representative realization. ASPHALT destabilizes itself once the surface switches to snow (indicated by the gray vertical dashed line). PROPOSED achieves better tracking performance than SNOW, despite SNOW using the correct stiffness and inertial values after the surface switch. However, note that the objective in the MPC formulation does not only consider lateral tracking error. When comparing PROPOSED with STIFFNESS, which uses the nominal inertial parameters, it is clear that estimating the inertial parameters indeed has benefits. The ASPHALT controller is unable to safely navigate the maneuvers on snow, and the SNOW controller behaves conservatively on asphalt. Both PROPOSED and STIFFNESS overshoot the first maneuver on snow, but are able to match the performance of the SNOW and ORACLE controllers once they have learned about the surface change.

Table I shows the results for 100 Monte-Carlo runs. Due to the nature of the maneuver, ASPHALT destabilized the vehicle in every execution when entering snow, so its results are summed up to the point of divergence. PROPOSED outperforms STIFFNESS (33%) and the snow models (37%) in terms of average cost, which shows the benefits with introducing active inertial-parameter estimation, at least for this particular maneuver.

VI. CONCLUSION

We extended a previously developed PF-based tire-stiffness estimator to relax the assumption of having known inertial parameters. Our simulation results show clear benefits with introducing inertial-parameter estimation into the tire-stiffness estimation, as the parameters are dependent on each other. While the exact knowledge of the inertial parameters is secondary for vehicle stability, the tracking error and objective function cost are clearly improved.

REFERENCES

[1] J. Svendenius, "Tire modeling and friction estimation," Ph.D. dissertation, Dept. Automatic Control, Lund University, Sweden, Apr. 2007.

[2] S. Solmaz, M. Akar, R. Shorten, and J. Kalkkuhl, "Real-time multiple-model estimation of centre of gravity position in automotive vehicles," *Veh. Syst. Dyn.*, vol. 46, no. 9, pp. 763–788, 2008.

[3] P. Falcone, F. Borrelli, J. Asgari, H. E. Tseng, and D. Hrovat, "Predictive active steering control for autonomous vehicle systems," *IEEE Trans. Control Syst. Technol.*, vol. 15, no. 3, pp. 566–580, 2007.

[4] R. Quirynen, K. Berntorp, and S. Di Cairano, "Embedded optimization algorithms for steering in autonomous vehicles based on nonlinear model predictive control," in *Amer. Control Conf.*, Milwaukee, WI, Jun. 2018.

[5] K. Berntorp, R. Quirynen, T. Uno, and S. Di Cairano, "Trajectory tracking for autonomous vehicles on varying road surfaces by friction-adaptive nonlinear model predictive control," *Veh. Syst. Dyn.*, vol. 58, no. 5, pp. 705–725, 2019.

[6] K. Berntorp and S. Di Cairano, "Tire-stiffness and vehicle-state estimation based on noise-adaptive particle filtering," *IEEE Trans. Control Syst. Technol.*, vol. 27, no. 3, pp. 1100–1114, 2018.

[7] R. Quirynen and S. Di Cairano, "PRESAS: Block-structured preconditioning of iterative solvers within a primal active-set method for fast model predictive control," *Optimal Control Applications and Methods*.

[8] R. Quirynen, M. Vukov, M. Zanon, and M. Diehl, "Autogenerating microsecond solvers for nonlinear MPC: a tutorial using ACADO integrators," *Optimal Control Applications and Methods*, vol. 36, pp. 685–704, 2014.

[9] A. Vahidi, A. Stefanopoulou, and H. Peng, "Recursive least squares with forgetting for online estimation of vehicle mass and road grade: theory and experiments," *Vehicle System Dynamics*, vol. 43, no. 1, pp. 31–55, 2005.

[10] F. Gustafsson, "Slip-based tire-road friction estimation," *Automatica*, vol. 33, pp. 1087–1099, 1997.

[11] C. Lundquist and T. B. Schön, "Recursive identification of cornering stiffness parameters for an enhanced single track model," in *15th IFAC Symp. System Identification*, Saint-Malo, France, Jul. 2009.

[12] C. Sierra, E. Tseng, A. Jain, and H. Peng, "Cornering stiffness estimation based on vehicle lateral dynamics," *Veh. Syst. Dyn.*, vol. 44, no. 1, pp. 24–38, 2006.

[13] K. Berntorp, B. Olofsson, K. Lundahl, and L. Nielsen, "Models and methodology for optimal trajectory generation in safety-critical road–vehicle manoeuvres," *Veh. Syst. Dyn.*, vol. 52, no. 10, pp. 1304–1332, 2014.

[14] F. Gustafsson, *Statistical Sensor Fusion*. Lund, Sweden: Utbildningshuset/Studentlitteratur, 2010.

[15] A. Doucet and A. M. Johansen, "A tutorial on particle filtering and smoothing: Fifteen years later," in *Handbook of Nonlinear Filtering*, D. Crisan and B. Rozovsky, Eds. Oxford University Press, 2009.

[16] C. M. Bishop, *Pattern Recognition and Machine Learning*. NJ, USA: Springer-Verlag New York, 2006.

[17] K. P. Murphy, "Conjugate Bayesian analysis of the Gaussian distribution," UBC, Tech. Rep., 2007.

[18] S. Vaskov, K. Berntorp, and R. Quirynen, "Cornering stiffness adaptive, stochastic nonlinear model predictive control for vehicles," in *Amer. Control Conf.*, New Orleans, LA, May 2021.

[19] M. Diehl, R. Findeisen, F. Allgöwer, H. G. Bock, and J. P. Schlöder, "Nominal stability of the real-time iteration scheme for nonlinear model predictive control," *IEE Proc.-Control Theory Appl.*, vol. 152, no. 3, pp. 296–308, 2005.

[20] H. B. Pacejka, *Tire and Vehicle Dynamics*, 2nd ed. Oxford, United Kingdom: Butterworth-Heinemann, 2006.